McNeill, L.C., Dugan, B., Petronotis, K.E., and the Expedition 362 Scientists
Proceedings of the International Ocean Discovery Program Volume 362
publications.iodp.org

https://doi.org/10.14379/iodp.proc.362.201.2019

Check for updates

Contents

Data report: $^{87}Sr/^{86}Sr$ in pore fluids from Expedition 362[1]

Morgan McCarthy,[2] Breeanna Zirkle,[2] Marta E. Torres,[2] and Brian A. Haley[2]

Keywords: International Ocean Discovery Program, IODP, *JOIDES Resolution*, Expedition 362, Site U1480, Site U1481, Sumatra Subduction Zone, Sr ratio, pore fluid

Abstract

We report on the Sr isotopic composition of pore fluids recovered from Sites U1480 and U1481 drilled during International Ocean Discovery Program Expedition 362, which sampled the incoming sedimentary section of North Sumatra to investigate the causes of shallow seismogenesis in the Sumatra-Andaman margin. Sr isotope data are valuable in identifying diagenetic alteration of the incoming sequence, which can alter mechanical properties of the sedimentary wedge and subsequently affect its seismogenic behavior. Site U1480 recovered input sediment to ~1420 meters below seafloor (mbsf), and sediment was sampled from 1150 to 1500 mbsf at Site U1481. To determine the Sr isotopic composition, acidified pore fluid samples recovered at sea were loaded directly onto columns containing EICHROM Sr-Spec resin and followed by analyses using a NU multicollector inductively coupled plasma–mass spectrometer (MC-ICPMS). We observed a marked increase in $^{87}Sr/^{86}Sr$ ratios to 0.71376 in the Sr contribution from alteration of terrigenous material from the Bengal-Nicobar Fan. This trend is reversed in the deeper sequence, where $^{87}Sr/^{86}Sr$ ratios decrease to 0.70820 in the deepest sample analyzed (1300 mbsf). Only the deepest sediment was recovered at Site U1481, and the pore fluids also show a decrease in $^{87}Sr/^{86}Sr$ ratios from 0.71296 at 1172 mbsf to 0.70913 at 1495 mbsf.

Introduction

International Ocean Discovery Program (IODP) Expedition 362 was designed to establish initial and evolving properties of the North Sumatran incoming sedimentary section and determine their role in shallow seismogenesis and forearc plateau development. The thick input section has likely undergone diagenetic alterations that may modify the mechanical properties of the wedge and so may promote shallow seismogenic slip. Fluids and associated diagenetic reactions are thus a key component of this study. The concentration of dissolved species and their isotopic composition provide critical data for the identification of fluid–rock reactions, the assessment of the potential role of fluid flow through the underlying oceanic crust, and the identification of any potential migration pathways and fluid sources (see review in Kastner et al., 2014).

During the fractional crystallization that took place early in our planet's history, incompatible elements like Rb were excluded from basaltic melts and incorporated into silicic residues (continental crust), which developed with a larger Rb/Sr ratio than the upper mantle. The isotopic composition of Sr has been changing through time as the radiogenic ^{87}Sr isotope is produced by emission of a negative β-particle from ^{87}Rb (Faure and Powell, 1972). Because of this, ^{87}Sr enrichment is high in old continental rocks (granites) and low $^{87}Sr/^{86}Sr$ ratios are found in the mantle and rocks derived from it (basalts). Marine sedimentary material reflects the seawater composition at the time of deposition, which in turn depends on the relative inputs from different weathering and hydrothermal sources. Different source materials are characterized by different Sr isotope signatures, which are not affected by biologically induced fractionations (e.g., Teichert et al., 2005; Torres et al., 2015); therefore, changes in concentration and isotopic composition of Sr in the pore water of marine sediment are powerful tracers for identifying fluid–rock reactions and the source of migrating fluids. Source materials responsible for enrichment in Sr concentration and for the alteration of its isotopic composition in interstitial water are continental detritus ($^{87}Sr/^{86}Sr$ = ~0.7119–0.7133), biogenic calcite ($^{87}Sr/^{86}Sr$ = ~0.7075–0.7092), volcanic material ($^{87}Sr/^{86}Sr$ = ~0.7065), oceanic crust ($^{87}Sr/^{86}Sr$ = ~0.703) and mixing with present-day seawater ($^{87}Sr/^{86}Sr$ = ~0.70917) or coeval seawater (e.g., Elderfield, 1986; Veizer, 1989). Here we report on analyses of Sr isotopes of pore fluids collected at Sites U1480 and U1481 during Expedition 362 to the Sumatra subduction zone.

Study sites

During Expedition 362, sediment was recovered to a maximum depth of 1500 meters below seafloor (mbsf) at Sites U1480 and

[1] McCarthy, M., Zirkle, B., Torres, M.E., Haley, B.A., 2019. Data report: $^{87}Sr/^{86}Sr$ in pore fluids from Expedition 362. *In* McNeill, L.C., Dugan, B., Petronotis, K.E., and the Expedition 362 Scientists, *Sumatra Subduction Zone*. Proceedings of the International Ocean Discovery Program, 362: College Station, TX (International Ocean Discovery Program). https://doi.org/10.14379/iodp.proc.362.201.2019

[2] College of Earth, Ocean and Atmospheric Science, Oregon State University, USA. Correspondence author: **mtorres@coas.oregonstate.edu**

MS 362-201: Received 13 July 2018 · Accepted 5 October 2018 · Published 30 January 2019

U1481, which were drilled on the Indian oceanic plate ~250 km southwest of the subduction zone (Figure **F1**). Data on the succession of sampled sediment and rock can be used to extrapolate how their properties evolve with burial as the sediment section thickens before reaching the subduction zone and how this modifies the sediment properties and influences fault slip behavior during earthquakes. A detailed description of the results can be found in the **Site U1480** and **Site U1481** chapters (McNeill et al., 2017b, 2017c).

Site U1480

Drilling at Site U1480 (3°2.04′N, 91°36.35′E; 4148 m water depth) recovered sediment and sedimentary rocks from the seafloor to 1415.3 mbsf (Figure **F2**). This complete sedimentary section is composed of Late Cretaceous to recent deep-marine sedimentary cover. Lithostratigraphic Units I and II (0–1250.3 mbsf) are composed of Nicobar Fan sedimentation and contain a range of siliciclastic turbidite deposits with varying amounts of carbonate and biosiliceous components. The detrital component, which is similar to the sediment gravity-flow deposits of the Bengal Fan, has been attributed to sources in the Himalayan-derived Ganges-Brahmaputra river system, Indo-Burman range/West Burma, and Sunda forearc and arc. The limited arc-derived ash content in these units suggests that the Sunda forearc constitutes only a minor sediment source (McNeill et al., 2017d).

Lithostratigraphic Units III–V (1250.35–1349.8 mbsf) are intervals dominated by pelagic sedimentation with significantly reduced sediment accumulation rates (McNeill et al., 2017d). Unit III (1250.3–1327.2 mbsf) shows a marked increase in lithification relative to overlying Unit II and is defined by an absence of micaceous quartzofeldspathic silt and sand. The upper sediment in this unit is dominated by gray-green and minor reddish brown claystone with agglutinated foraminifers and overlies a sequence of reddish brown tuffaceous silty claystone with biosiliceous debris and minor chalk. Unit IV (1327.2–1349.8 mbsf) is composed of basaltic flows, tuffaceous and volcaniclastic sandstone, and volcanic breccia. Unit V (1349.8–1415.3 mbsf) is defined mainly on the appearance of calcareous claystone and chalk and intercalated magmatic intrusions. Beneath the sedimentary cover, igneous extrusive and intrusive rocks are interbedded with volcaniclastic sediment and underlain by a thin interval (1415.3–1431.6 mbsf) of basaltic crustal rock of the igneous basement (Unit VI).

Site U1481

Site U1481 (2°45.29′N, 91°45.58′E; 4178 m water depth) is located 35 km southeast of Site U1480. Drilling at this site recovered sediment from 1150 mbsf to within a few tenths of meters from basement at 1500 mbsf. The goal was to determine if the lower sediment section and basement at Site U1480 are representative of this

Figure F1. A. Regional map of study area with location of drilled sites, 2004 earthquake rupture area, and Bengal-Nicobar Fan system. Dashed square = location of B. GR = Ganges River, IBR = Indo-Burman range (modified from McNeill et al., 2017d). B. Multichannel seismic reflection profiles across the North Sumatran forearc (location of the southern 2004 earthquake rupture zone) and Indian oceanic plate overlain on multibeam bathymetry. C. Site U1480 on seismic profile Line BGR06-101–102 (see B). Blue line = unconformity between the trench wedge and underlying Nicobar Fan sediments, green line = transition from reflective to less reflective stratigraphy, dashed red line = high-amplitude reflector with negative polarity toward the subduction zone (modified from McNeill et al., 2017b, based on data from McNeill et al., 2016). D. Site U1481 on seismic profile Line BGR06-103 (see B; modified from McNeil et al., 2017c, based on data from McNeill et al., 2016).

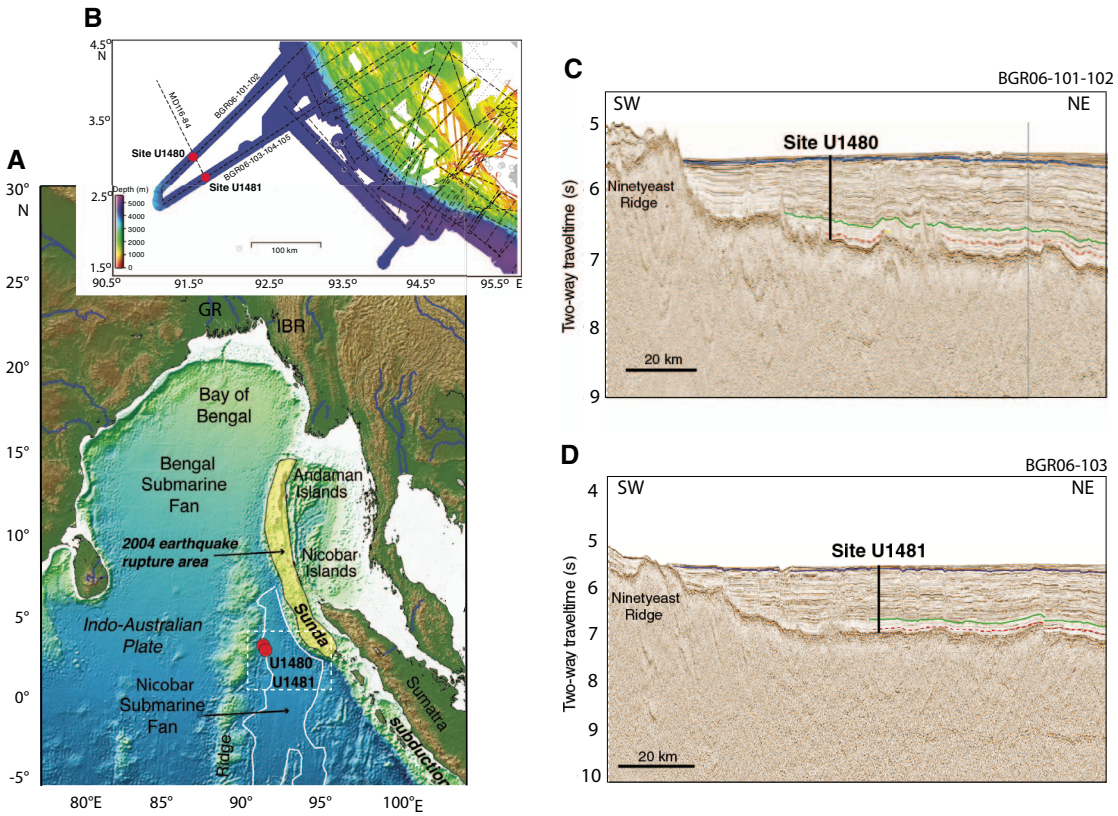

Figure F2. Sr concentration and isotopic ratios measured in pore fluid from Sites U1480 (blue) and U1481 (red). Lithostratigraphic units and ages correspond to those from the Site U1480 and Site U1481 chapters (McNeill et al., 2017b, 2017c). Enrichment in $^{87}Sr/^{86}Sr$ relative to the seawater (SW; arrow) ratio of 0.7092 is evidence for weathering of continentally derived silicates that release this radiogenic isotope. The decrease in $^{87}Sr/^{86}Sr$ ratios in the deepest samples suggests a contribution from Sr released by alteration of basement.

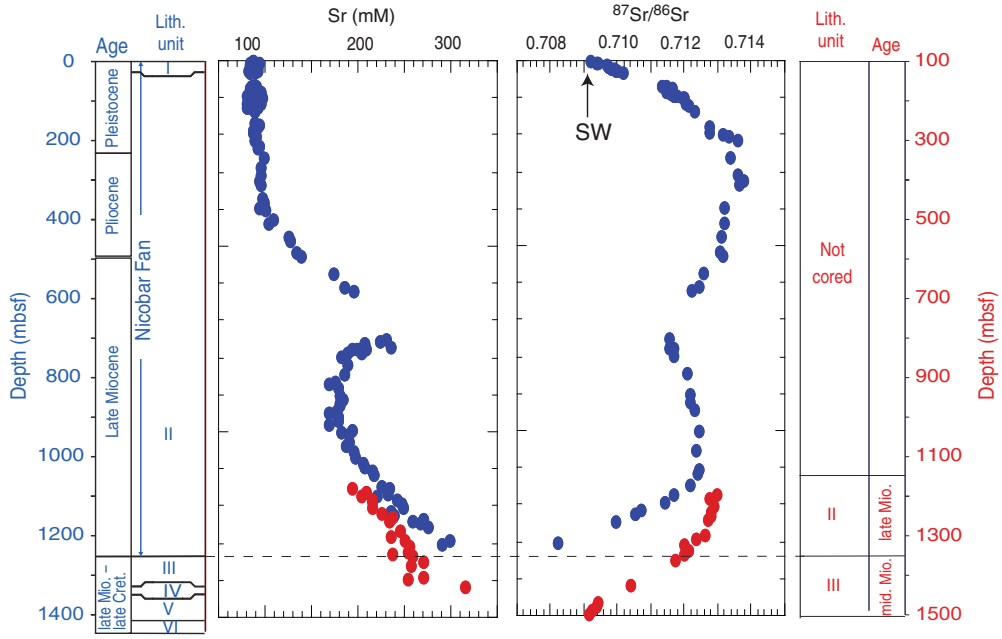

part of the Indian plate and therefore evaluate the degree of heterogeneity of sediment and basement over short distances (see the **Site U1481** chapter; McNeill et al., 2017c).

The sediment sequence recovered at Site U1481 consists of siliciclastic sediment interpreted as the older stratigraphic part of the last active Nicobar Fan and the underlying hemipelagic to pelagic sediment equivalent to the material recovered between 785.8 and 1310.1 mbsf (lithostratigraphic Subunits IIC and IIIA) at Site U1480. Because of time constraints, drilling into the underlying deepest prefan pelagic sediment and basement was not possible.

Analytical methods

Pore fluids were collected from whole-round cores that were cut on the catwalk immediately after recovery, capped, and taken to the laboratory for processing using a titanium squeezer modified after the stainless-steel squeezer of Manheim and Sayles (1974). Details on sampling protocols are given in the **Expedition 362 methods** chapter [McNeill et al., 2017a]). Dissolved Sr concentrations were measured on board using an inductively coupled plasma–atomic emission spectrometer (ICP-AES) with a Teledyne Prodigy high-dispersion instrument. Samples were diluted 20-fold using ultrapure nitric acid (2%), and concentrations were determined from calibration curves using matrix-matched standards, with an average precision better than 1% (see the **Expedition 362 methods** chapter [McNeill et al., 2017a])

For isotopic analyses, Sr separation was achieved by loading aliquots containing ~300 ng of Sr on a 50 µL Sr-specific column and resin from EICHROM. Samples from the columns were collected in acid-washed polytetrafluoroethylene bottles and acidified with 2 mL of 3% HNO_3. Isotopic analysis was performed using the Nu Plasma multicollector inductively coupled–mass spectrometer (MC-ICPMS) housed in the W.M. Keck Collaboratory for Plasma Spectrometry at Oregon State University (Ross et al., 2015). $^{87}Sr/^{86}Sr$ ratios were normalized to the National Bureau of Standards 987 standard, with an $^{87}Sr/^{86}Sr$ ratio of 0.71025 ± 0.00005 (2σ mean; N = 91). External error is represented through replicate analysis of an in-house standard with an $^{87}Sr/^{86}Sr$ ratio of 0.708170 ± 0.000051 (2σ mean; N = 91).

Results

From the 168 pore fluid samples for which there were dissolved Sr data available, $^{87}Sr/^{86}Sr$ isotope ratios were measured in 77 samples (Table **T1**). This data set reflects the availability of pore fluid subsamples for $^{87}Sr/^{86}Sr$ analyses, which was limited by the volume of fluid recovered and the broad spectrum of desired postcruise analyses. The downcore distribution of dissolved Sr and its isotopic composition is shown in Figure **F2**.

At Site U1480, Sr concentrations remain relatively consistent around 80–100 µM (approximately the concentration of seawater) at 0–300 mbsf (Figure **F2**). $^{87}Sr/^{86}Sr$ ratios increase from a near-seawater ratio of 0.709195 at 1.40 mbsf to 0.71364 at 336 mbsf, a depth interval that corresponds to the Pliocene–Pleistocene deposits of the Nicobar Fan. This marked increase in the Sr radiogenic signal points to alteration of the reactive siliciclastic component in the turbidite deposits, which is thought to originate from erosion of the Himalaya and Tibetan Plateau. Chemical changes in dissolved pore fluid components measured on board were used to suggest alteration of volcaniclastics with an overall decrease in the concentration of K, Li, and B and a release of Ca (see the **Site U1480** chapter [McNeill et al., 2017b]), which is commonly observed in ash-bearing sediment (e.g., Gieskes and Lawrence, 1981; Lawrence and Gieskes, 1981). However, the isotopic data presented here clearly points to alteration of detrital (rather than volcanogenic) silicates, which is similar to previously documented alteration of continentally de-

Table T1. Pore fluid strontium concentration and $^{87}Sr/^{86}Sr$ ratios, Sites U1480 and U1481. **Download table in CSV format.**

Figure F3. $^{87}Sr/^{86}Sr$ isotope ratios versus the inverse of Sr concentration, Sites U1480 (blue) and U1481 (red). Triangles = data from shallower than 300 mbsf, squares = data from 300 to 1100 mbsf, diamonds = data from deeper than 1100 mbsf. Only data deeper than 1100 mbsf were collected for Site U1481. Arrows point toward increasing sediment depths.

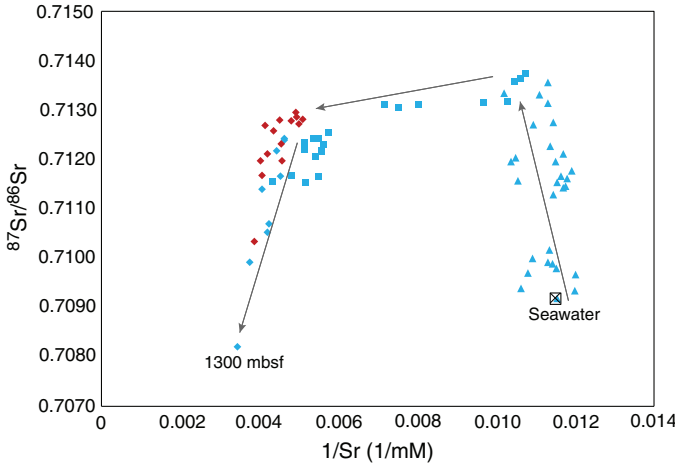

rived material in sediment recovered from the Indian margin and the Ulleung Basin (Solomon et al., 2014; Kim et al., 2016).

The trend toward radiogenic Sr displays an inflection at 336 mbsf, where $^{87}Sr/^{86}Sr$ ratios decrease from 0.71364 to 0.71167 at 794 mbsf, a depth that corresponds to a marked increase in dissolved Sr concentration and may be related to carbonate diagenesis (see the **Site U1480** chapter [McNeill et al., 2017b]). Between 794 and 1115 mbsf, a second broad maximum in $^{87}Sr/^{86}Sr$ ratios (0.71243 at 1107 mbsf) possibly reflects marine silicate diagenesis in the lowermost Nicobar Fan deposits. This trend is reversed toward the bottom of the sediment section, with the lowest $^{87}Sr/^{86}Sr$ ratio (0.70820) occurring in the deepest pore water sample available (1300 mbsf). Pore fluid characteristics in these deepest lithostratigraphic units (III–V) are indicative of alteration reactions in oceanic basement (see the **Site U1480** chapter [McNeill et al., 2017b]).

Drilling at Site U1481 only recovered the older stratigraphic section of the Nicobar Fan and the underlying hemipelagic to pelagic sediment (see the **Site U1481** chapter [McNeill et al., 2017c]). Sr concentration data from the cored section shows a general increase with depth from 1160 mbsf (194.6 µM) that corresponds to the increase in Sr observed with depth at Site U1480 (Figure **F2**). Consistent with the data obtained at Site U1480, isotopic ratios at Site U1481 decrease from an $^{87}Sr/^{86}Sr$ ratio of 0.712965 at 1172 mbsf to 0.70913 at the bottom of the recovered section (1495 mbsf).

The relationship between the isotopic ratios at Sites U1480 and U1481 and their inverse Sr concentration (1/Sr) is shown in Figure **F3**. The figure separates data from Site U1480 into three depth intervals: 0–300 mbsf (blue triangles), 300–1100 mbsf (blue squares), and samples deeper than 1100 mbsf (blue diamonds). For Site U1481, data are only available from deeper than 1100 mbsf (red diamonds). This figure shows a well-defined mixing relationship for the composition of samples in the upper 300 mbsf, which varies from seawater values (marked with X) and have a progressive alteration signal for the Nicobar Fan detrital siliciclastics. The deepest sediment (deeper than 1100 mbsf) at both sites define a mixing regime from a diagenetic pore water signal toward a component of the fluids that is indicative of basement alteration reactions. Not surprisingly, the lowest $^{87}Sr/^{86}Sr$ ratio was measured in the deepest sample recovered from Site U1480; drilling at Site U1481 terminated before basement was reached.

Acknowledgments

This research used samples and data provided by the International Ocean Discovery Program (IODP). The outstanding efforts of the Siem Offshore officers and crew, the drilling personnel, and the scientific party of IODP Expedition 362 are greatly acknowledged here; without their hard work and dedication none of these samples could have been recovered for analysis. Funding for this research was provided by the IODP U.S. Science Support Program Office (National Science Foundation prime award OCE-1450528) to M.E. Torres.

References

Elderfield, H., 1986. Strontium isotope stratigraphy. *Palaeogeography, Palaeoclimatology, Palaeoecology,* 57(1):71–90. **https://doi.org/10.1016/0031-0182(86)90007-6**

Faure, G., and Powell, J.L., 1972. *Strontium Isotope Geology:* New York (Springer-Verlag). **https://doi.org/10.1007/978-3-642-65367-4**

Gieskes, J.M., and Lawrence, J.R., 1981. Alteration of volcanic matter in deep-sea sediments: evidence from the chemical composition of interstitial waters from deep sea drilling cores. *Geochimica et Cosmochimica Acta,* 45(10):1687–1703. **https://doi.org/10.1016/0016-7037(81)90004-1**

Kastner, M., Solomon, E.A., Harris, R.N., and Torres, M.E., 2014. Fluid origins, thermal regimes, and fluid and solute fluxes in the forearc of subduction zones. *In* Stein, R., Blackman, D., Inagaki, F., and Larsen, H.-C., *Developments in Marine Geology* (Volume 7): *Earth and Life Processes Discovered from Subseafloor Environments: a Decade of Science Achieved by the Integrated Ocean Drilling Program (IODP).* R. Stein (Series Ed.): Amsterdam (Elsevier B.V.), 671–733. **https://doi.org/10.1016/B978-0-444-62617-2.00022-0**

Kim, J.-H., Torres, M.E., Haley, B.A., Ryu, J.-S., Park, M.-H., Hong, W.-L., and Choi, J., 2016. Marine silicate weathering in the anoxic sediment of the Ulleung Basin: evidence and consequences. *Geochemistry, Geophysics, Geosystems,* 17(8):3437–3453. **https://doi.org/10.1002/2016GC006356**

Lawrence, J.R., and Gieskes, J.M., 1981. Constraints on water transport and alteration in the oceanic crust from the isotopic composition of pore water. *Journal of Geophysical Research: Solid Earth,* 86(B9):7924–7934. **https://doi.org/10.1029/JB086iB09p07924**

Manheim, F.T., and Sayles, F.L., 1974. Composition and origin of interstitial waters of marine sediments, based on deep sea drill cores. *In* Goldberg, E.D. (Ed.), *The Sea* (Volume 5): *Marine Chemistry: The Sedimentary Cycle:* New York (Wiley), 527–568.

McNeill, L., Dugan, B., and Petronotis, K., 2016. *Expedition 362 Scientific Prospectus Addendum: the Sumatra subduction zone.* International Ocean Discovery Program. **https://doi.org/10.14379/iodp.sp.362add.2016**

McNeill, L.C., Dugan, B., Petronotis, K.E., Backman, J., Bourlange, S., Chemale, F., Chen, W., Colson, T.A., Frederik, M.C.G., Guèrin, G., Hamahashi, M., Henstock, T., House, B.M., Hüpers, A., Jeppson, T.N., Kachovich, S., Kenigsberg, A.R., Kuranaga, M., Kutterolf, S., Milliken, K.L., Mitchison, F.L., Mukoyoshi, H., Nair, N., Owari, S., Pickering, K.T., Pouderoux, H.F.A., Yehua, S., Song, I., Torres, M.E., Vannucchi, P., Vrolijk, P.J., Yang, T., and Zhao, X., 2017a. Expedition 362 methods. *In* McNeill, L.C., Dugan, B., Petronotis, K.E., and the Expedition 362 Scientists, *Sumatra Subduction Zone.* Proceedings of the International Ocean Discovery Program, 362: College Station, TX (International Ocean Discovery Program). **https://doi.org/10.14379/iodp.proc.362.102.2017**

McNeill, L.C., Dugan, B., Petronotis, K.E., Backman, J., Bourlange, S., Chemale, F., Chen, W., Colson, T.A., Frederik, M.C.G., Guèrin, G., Hama-

hashi, M., Henstock, T., House, B.M., Hüpers, A., Jeppson, T.N., Kachovich, S., Kenigsberg, A.R., Kuranaga, M., Kutterolf, S., Milliken, K.L., Mitchison, F.L., Mukoyoshi, H., Nair, N., Owari, S., Pickering, K.T., Pouderoux, H.F.A., Yehua, S., Song, I., Torres, M.E., Vannucchi, P., Vrolijk, P.J., Yang, T., and Zhao, X., 2017b. Site U1480. *In* McNeill, L.C., Dugan, B., Petronotis, K.E., and the Expedition 362 Scientists, *Sumatra Subduction Zone.* Proceedings of the International Ocean Discovery Program, 362: College Station, TX (International Ocean Discovery Program). **https://doi.org/10.14379/iodp.proc.362.103.2017**

McNeill, L.C., Dugan, B., Petronotis, K.E., Backman, J., Bourlange, S., Chemale, F., Chen, W., Colson, T.A., Frederik, M.C.G., Guèrin, G., Hamahashi, M., Henstock, T., House, B.M., Hüpers, A., Jeppson, T.N., Kachovich, S., Kenigsberg, A.R., Kuranaga, M., Kutterolf, S., Milliken, K.L., Mitchison, F.L., Mukoyoshi, H., Nair, N., Owari, S., Pickering, K.T., Pouderoux, H.F.A., Yehua, S., Song, I., Torres, M.E., Vannucchi, P., Vrolijk, P.J., Yang, T., and Zhao, X., 2017c. Site U1481. *In* McNeill, L.C., Dugan, B., Petronotis, K.E., and the Expedition 362 Scientists, *Sumatra Subduction Zone.* Proceedings of the International Ocean Discovery Program, 362: College Station, TX (International Ocean Discovery Program). **https://doi.org/10.14379/iodp.proc.362.104.2017**

McNeill, L.C., Dugan, B., Backman, J., Pickering, K.T., Pouderoux, H.F.A., Henstock, T.J., Petronotis, K.E., et al., 2017d. Understanding Himalayan erosion and the significance of the Nicobar Fan. *Earth and Planetary Science Letters,* 475:134–142. **https://doi.org/10.1016/j.epsl.2017.07.019**

Ross, N., Torres, M.E., Haley, B.A., Solomon, E.A., and Kastner, M., 2015. Data report: strontium isotope analyses of pore fluids from the CRISP-A transect drilled during Expeditions 334 and 344. *In* Harris, R.N., Sakaguchi, A., Petronotis, K., and the Expedition 344 Scientists, *Proceedings of the Integrated Ocean Drilling Program,* 344: Tokyo (Integrated Ocean Drilling Program Management International, Inc.). **https://doi.org/10.2204/iodp.proc.344.201.2015**

Solomon, E.A., Spivack, A.J., Kastner, M., Torres, M.E., and Robertson, G., 2014. Gas hydrate distribution and carbon sequestration through coupled microbial methanogenesis and silicate weathering in the Krishna–Godavari Basin, offshore India. *Marine and Petroleum Geology,* 58(A):233–253. **https://doi.org/10.1016/j.marpetgeo.2014.08.020**

Teichert, B.M.A., Torres, M.E., Bohrmann, G., and Eisenhauer, A., 2005. Fluid sources, fluid pathways and diagenetic reactions across an accretionary prism revealed by Sr and B geochemistry. *Earth and Planetary Science Letters,* 239(1–2):106–121. **https://doi.org/10.1016/j.epsl.2005.08.002**

Torres, M.E., Cox, T., Hong, W.-L., McManus, J., Sample, J.C., Destrigneville, C., Gan, H.M., Gan, H.Y., and Moreau, J.W., 2015. Crustal fluid and ash alteration impacts on the biosphere of Shikoku Basin sediments, Nankai Trough, Japan. *Geobiology,* 13(6):562–580. **https://doi.org/10.1111/gbi.12146**

Veizer, J., 1989. Strontium isotopes in seawater through time. *Annual Review of Earth and Planetary Sciences,* 17(1):141–167. **https://doi.org/10.1146/annurev.ea.17.050189.001041**